NASA Contractor Report 202306

Potential New Sensor for Use With Conventional Gas Carburizing

W.A. de Groot
NYMA Inc.
Brook Park, Ohio

January 1997

Prepared for
Lewis Research Center
Under Contract NAS3–27186

National Aeronautics and
Space Administration

Potential New Sensor for Use with Conventional Gas Carburizing

W.A. de Groot
NYMA Inc., Brook Park, Ohio

Abstract

Diagnostics developed for in-situ monitoring of rocket combustion environments have been adapted for use in heat treating furnaces. Simultaneous, in-situ monitoring of the carbon monoxide, carbon dioxide, methane, water, nitrogen and hydrogen concentrations in the endothermic gas of a heat treating furnace has been demonstrated under a Space Act Agreement between NASA Lewis, the Heat Treating Network, and Akron Steel Treating Company. Equipment installed at the Akron Steel Treating Company showed the feasibility of the method. Clear and well-defined spectra of carbon monoxide, nitrogen and hydrogen were obtained by means of an optical probe mounted on the endothermic gas line of a gas generator inside the plant, with the data reduction hardware located in the basement laboratory. Signals to and from the probe were transmitted via optical fibers.

Background

The carbon potential of a carrier gas in the heat treating industry is defined as the degree to which a protective atmosphere provides carbon for absorption. It depends on the composition of the gaseous atmosphere and on the temperature of the furnace.[1,2] Most heat treating operations use an endothermic gas as protective atmosphere. This endothermic gas is created in a generator and consists of a mixture of approximately 20% carbon monoxide (CO), 40% nitrogen (N_2), and 40% hydrogen (H_2). Small amounts of hydrocarbons or air can be added to this endothermic gas upon entering the furnace in order to increase or decrease the available carbon.[2] The composition of the endothermic gas is critical to the quality of the finished product.

The working principle of most endothermic gas generators is based on passing a mixture of natural gas and air over a heated catalyst. The combination of heat and catalyst converts the air and natural gas into the endothermic gas mixture (a purely catalytic reaction, no combustion). The composition of this endothermic gas, and the percentages of carbon monoxide and methane critical for carburization, varies as a result of fluctuations in composition of the natural gas supply, gas/air ratio, the condition of the catalyst bed, and other variables. This in turn leads to a variation in carbon potential which could lead to an unacceptable quality of the steel product.

Adequate monitoring and control of the gas composition of the protective atmosphere is required to ensure product quality. Because a direct relationship exists between dewpoint, furnace temperature, and carbon potential, it is possible to determine the carbon potential by measuring the other two variables. No accurate determination of the dewpoint inside the furnace has been available, however, and oxygen probes have replaced dewpoint techniques as a control system to provide a stable endothermic gas atmosphere.

Oxygen probes have a solid, but far from perfect performance record. Problems associated with the probes include their dependence on assuming a constant CO which might not be true, that soot presence local to the probe will distort the bulk reading, that the probe itself acts as a catalyst for the decomposition of hydrocarbons, that the reference atmosphere used is contaminated and as such will distort the reading, or that the electrode fails. These problems and a number of solutions to alleviate them or make them have less of an impact have been described elsewhere.[3]

A more accurate, but also significantly more capital intensive system is based on multiple-gas infrared (IR) detection systems. Infrared analyzers are very accurate, but have the disadvantage that they are costly and that the measurement does not occur in-situ. A sample of the gas needs to be extracted, filtered, and cooled. Depending on the

initial gas composition, changes might occur as the result of these sample preparation processes. It also increases the time between extraction of the sample and the actual measurement. Furthermore, infrared analyzers cannot detect all species present. Due to the molecular structure of oxygen, for example, this species does not have an infrared signature and cannot be measured with infrared techniques.

An alternate technique, proposed here, is Raman spectroscopy. It is closely related to infrared analysis and has the capability of detecting and identifying all polyatomic species, in-situ and real time.[4,5] The main disadvantage of the technique is that the signal generated by gases is very weak. Historically this weak signal precluded the use of the technique for process control, but recent developments in optics and electronics has brought the technique within reach of being developed for instrumentation and control. In combination with high power lasers and fiber optics, this technique can be applied for in-situ and real time measurements of gas flows. The advantage over the conventional methods is that several species can be monitored simultaneously. A second advantage is that the measurement is direct, without the need of assumptions, gas filtering, or in-line calibration. Finally, the probe will not wear or burn off due to high temperature exposure, because the probing occurs from a distance.

Diagnostics based on Raman spectroscopy were developed for in-situ monitoring of rocket combustion environments.[6-9] A compact instrument was developed, based on this technique, that originally was used to detect hydrogen leaks.[10,11] With a few minor modifications, this instrument was adapted to detect and monitor a number of species. Laboratory experiments with the device are described in which carbon monoxide, oxygen, nitrogen, and hydrogen are detected with a partial pressure of 0.2 psi, and carbon dioxide and methane with a partial pressure of 0.1 psi. The purpose of the instrument, however, is not to detect, identify and quantify the species present in the endogas but rather to monitor the concentrations of selected species. For the heat treating applications, the species determined to be important for carburization were carbon monoxide, carbon dioxide, methane, and water (which directly translates into dewpoint).

Results are given of a field test where the system was installed and operated on the endothermic gas generator in a steel treating plant in order to do in-situ, real time monitoring of the composition of the endothermic gas. Initial tests were done to determine the accuracy and response of the device. As a crucial test it was determined to only monitor the carbon monoxide concentration. Future improvements in sensitivity and response will allow carbon dioxide and methane to be monitored and will open the possibility of using this device to monitor the furnace atmosphere directly.

Basic Sensor Principle

Raman spectroscopy probes the internal molecular rotational/vibrational structure and in doing so recognizes the type of molecule. A detailed explanation of the principles is given in refs. 4 and 5. A summary description will be given here in the context of the instrument design.

The green light of an Argon Ion laser is focused onto the gas to be analyzed or monitored. The molecules in the gas scatter the light in many different wavelengths (colors). Some of these wavelengths depend on the type of molecules, through their internal energy structure. Collecting and analyzing the scattered radiation by wavelength gives information about the type and quantity of the species present. Real time analysis of the intensities at these wavelengths allows quantitative monitoring of the gas composition.

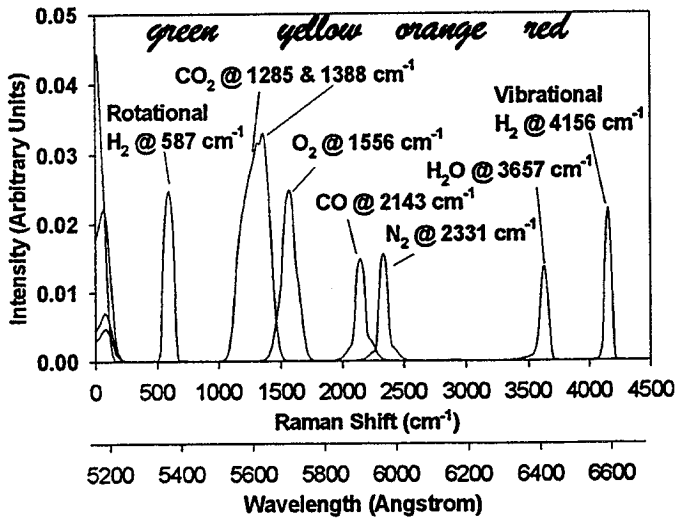

Fig. 1: Computed spectrum of species of interest.

An example spectrum, in which the wavelengths and intensities are shown where the different molecules will scatter the green light, is displayed in Figure 1. This computed Raman spectrum shows hydrogen (both "rotational" and "vibrational"), carbon dioxide, oxygen, carbon monoxide, nitrogen, and water for equal number densities. Computations assumed randomly polarized incident and collected radiation and a back scatter geometry, where the same lens that focuses the laser beam is used to collect the emitted light. The horizontal axis is expressed in wavenumbers, which are independent of the incident laser wavelength (color). A second axis is displayed which indicates the respective wavelengths in the case that an Argon Ion laser with a wavelength of 514.5 nm (green light) is used. The vertical axis displays the relative intensities of the emitted radiation. The colors of the light emitted by the

different species under exposure by the green light from an Argon Ion laser are shown at the top of the figure.

Each species shows a different intensity even though the number densities are equal. Several factors contribute to this variation. The most important factor is the transition probability which is the probability that the molecules undergo a specific transition upon being exposed to incident light. This factor is included in a relative intensity term called the scattering cross section, which can be obtained empirically for all gases. For a specific measurement system, a simple calibration can be performed that includes this term. Several methods are available to separate the different wavelengths, such as prisms, gratings, passband filters, and interferometers after which the intensities at each wavelength can be monitored.

An instrument has been designed that allows real-time, in-situ monitoring of the gas. It consists of an enclosure which houses a laser and the data acquisition equipment, and a small size (10 in^3) optical probe. The probe is connected to the housing by optical fibers, that transmit laser light to the probe and collected light, scattered from molecules, back to the data acquisition equipment. A schematic of the optical probe is given in Figure 2. A detailed description of the instrument is given in reference 10. The probe can be mounted on the endothermic gas line or other location to monitor gas compositions.

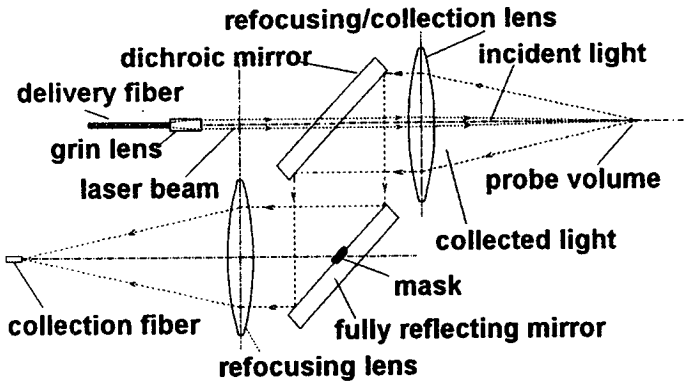

Fig. 2: Raman gas detection diagnostics probe schematic

Before the laser light is coupled into the delivery fiber, it is modulated with an optical chopper at about 400 Hz. The light scattered and collected also exhibits this modulation. The collected light is spectrally separated and detected with a photomultiplier tube. The PM tube signal is processed with a lock-in amplifier, which separates the modulated light from other light that contaminates the signal. The amplifier provides wavelength dependent intensities that are proportional to the gas species present.

Laboratory Tests

Before taking the instrument on a field test, laboratory tests were conducted to test the instrument under controlled conditions. The optical probe was mounted to a test vessel (Figure 3), with 12 ft optical fibers connecting the probe to the main instrument body. Gases analyzed were carbon dioxide, carbon monoxide, oxygen, nitrogen, methane, and hydrogen. For each of the above gases, a mixture of 50%/50% of nitrogen/sample gas at ambient temperature and pressure was placed inside the vessel. The scattered light was analyzed by scanning the visible spectrum with a spectrometer from 5145 to 6600 Angstrom (0 to 4500 cm^{-1}).

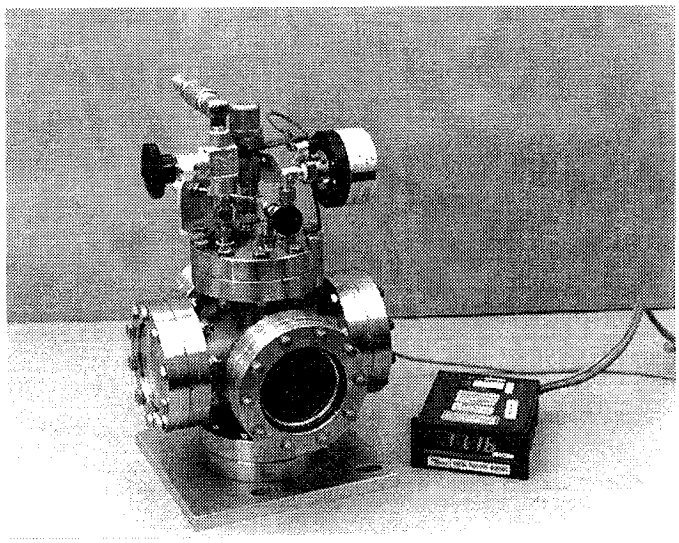

Fig. 3: Sample vessel for detection and monitoring of gaseous species

The results are shown in Figure 4. The insert shows the uncorrected spectra, with the horizontal axis showing the wavelength in wavenumbers, and the vertical axis showing the measured intensity. The main figure shows the spectra after background subtraction in post processing. The horizontal axis is converted to wavenumber, which indicates the distance from the laser line (this can be obtained by subtracting the inverse of the spectral location from the inverse of the laser wavelength in cm). The scan rate used to obtain each spectrum was 0.1 Angstrom/s. The time constant of the lock-in amplifier was 30 s. With this long time constant, the measurement is influenced by its history for up to 150 s (translating into 15 A). This causes each detected peak to be relatively broad, and the peak value to be smaller than the instantaneous peak value. However, by choosing this long time constant for the calibration, fluctuations are suppressed, while the relative peak strengths are still representative of the real peak height ratios.

The baseline of the uncorrected spectra (no background subtraction) shows steep slopes at the low (<1000 cm^{-1}) and high (>4000 cm^{-1}) wavenumber shifts. These gradients reflect the transmission curves of the dichroic filters and the laser notch filters and are caused by stray laser light, and by stimulated Raman and fluorescence phenomena inside the fibers. In this context it is important to realize that the shape of these slopes are strongly dependent on the length of the optical fibers. High intensity light passing through longer optical fibers induce larger fluorescence and stimulated Raman emission.

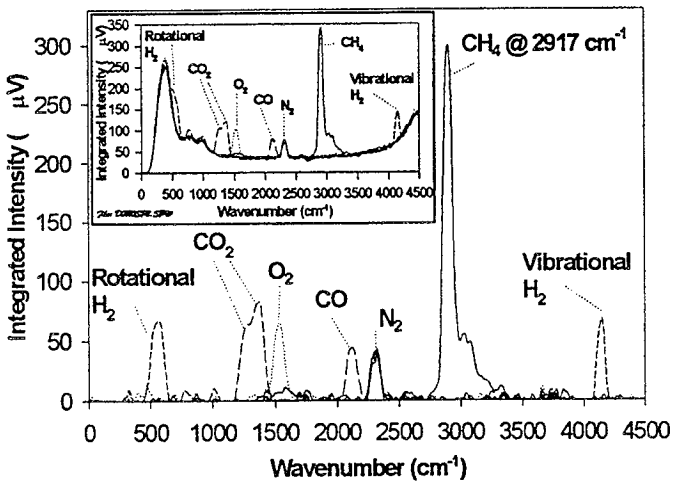

Fig. 4: Raman spectra of gaseous constituents in gas mixtures after background subtraction. Insert: Raw spectra before background subtraction.

The spectra of carbon dioxide at the low wavenumbers, and of hydrogen at the high wavenumbers are influenced by these slopes. They should be included in the data analysis, but a good characterization will ameliorate the problems arising from their existence. It might be possible to move the slopes to lower and higher wavenumbers by means of improved optics. That will be investigated. For now, the slopes will only be considered where they are of critical importance.

Figure 4 shows a baseline caused by system noise and stray laser light. Identifiable peaks are, from left to right, carbon dioxide (1285 cm^{-1} and 1388 cm^{-1}), oxygen (1556 cm^{-1}), carbon monoxide (2143 cm^{-1}), nitrogen (2331 cm^{-1}), methane (2917 cm^{-1}) and hydrogen (4156 cm^{-1}). Because carbon dioxide and methane consist of multiple atoms, they show multiple peaks. Carbon dioxide shows two peaks, and methane shows at least four peaks. However, for monitoring purposes, only the dominant peak is of interest. The other peaks have to be considered in order to verify their effect on the strength of other species' peaks. The pure rotational Raman spectrum of hydrogen is also resolved (587 cm^{-1}). But because it is located on the steep slope created by the filters and optical fibers, it is difficult to utilize for real-time measurements.

Table I: Measured Raman data of selected species

Peak Type	Theor. Ram. Shift (cm^{-1})	Exp. Ram. Shift (cm^{-1})	Spectr. Locat. (A)	Relat. Int. (N_2= 1.0)	Scat. Cross Sect. (Lit.)
H_2 Rot.	587	570	5300	1.67	
CO_2	1285 1388	1284 1373	5509 5536	1.59 2.05	0.7 (a) 1.2 (a)
O_2	1556	1531	5585	1.62	1.0 (a)
CO	2143	2117	5774	1.10	0.9 (a)
N_2	2331	2316	5841	1.00	1.0 (a)
CH_4	2917	2905	6049	7.47	9.1 (a)
H_2O	3652	(b)	(b)	(b)	3.4 (a)
H_2 Vib.	4156	4148	6541	1.69	3.4 (a)

(a) Schroetter, H.W., and Kloeckner, H.W., "Raman Scattering Cross Sections in Gases and Liquids," *Raman Spectroscopy of Gases and Liquids* (A. Weber, Ed.) Topics in Current Physics: Springer Verlag, 1979.

(b) Not measured in current laboratory tests

Figure 4 allows a first approximation of the relative signal strengths for the different species. Because the pressure and temperature of ambient air can easily be measured, nitrogen was used as the reference species with oxygen as a potential back-up. If the strength of the nitrogen signal is assumed to be unity (1.00), then the strength of the other species can be related to this value. The results are given in Table I, together with the Raman shift (in wavenumbers) and the corresponding spectral location of the peak, for the green light of an Argon-ion laser.

The measured Raman shifts are off by up to 26 Angstrom from values found in literature. This could be caused by instrument calibration inaccuracies (especially the spectrometer alignment) and by the correction for the time lag

in the lock-in detection, which might have been overcorrected. The two peaks of carbon dioxide convolute, and are extracted using deconvolution software to obtain the signal intensity. The experimental data from literature, given in the last column can only be used as a guideline, because these scattering cross sections are measured with specific polarization properties of the incident and observed light, and for a 90 degree angle of observation with respect to the laser propagation. The current instrument uses randomly polarized light and a back scatter geometry for observation. These data are used in the data reduction of the field tests at the steel treating plant.

Field Test

The instrument was taken to the Akron Steel Treating Company. Because no window was readily available inside the endothermic gas line, it was decided to install the previously used test vessel against the gas generator, as shown in Figure 5. A two feet long copper tube, equipped with a simple on-off valve, was connected between the endothermic gas line and the vessel, after the gas was cooled down. A second section of copper tubing was mounted to the vessel and transported the gas to the burn-off stack.

Because the endogas line operates at slightly higher than atmospheric pressure (~3.5 KPa higher), opening the valve was sufficient to let a small flow of the endogas pass through the vessel. The temperature of the gas at this point was not known, but estimated to be between 100 and 300 F. It was also not known how fast a change in the endogas composition will be fully reflected inside the vessel by replacing the gas inside the whole vessel volume. Thus a time lag between the change in concentration of the endogas and when this change is recorded by the instrument was partly due to this replacement volume inside the vessel.

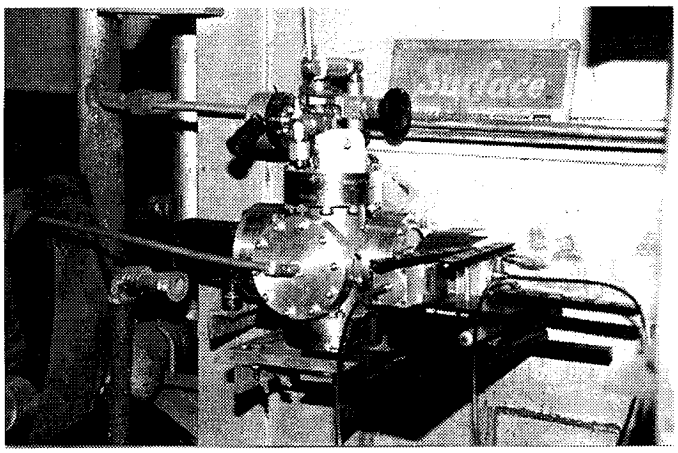

Fig. 5: Sample vessel with optical probe attached to endothermic gas generator

The optical probe was mounted to the vessel window, identical to the laboratory setup. Vibrations of the vessel and probe were not expected to have an effect on the monitoring, because of the conjugate nature of the back scatter optics. A calorimeter was mounted to the window opposite the probe to measure the intensity of the transmitted laser light and the low frequency fluctuations in light intensity.

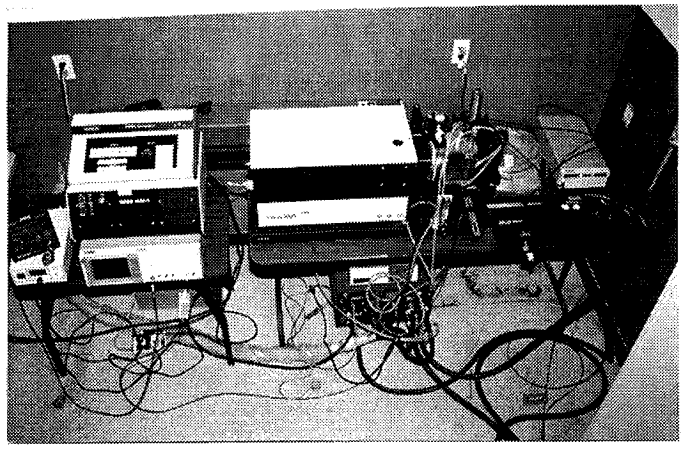

Fig. 6: Laser, data acquisition, and fiber coupling equipment installed in the basement laboratory.

The laser, laser fiber coupling and data acquisition and reduction equipment were installed in the basement laboratory, see Figure 6. From there, three 150 ft. fibers were installed which extended from the instrument, across a section of the factory floor and one floor up to the endothermic gas generator, where they were coupled to the optical probe. One fiber was used to transmit the incident laser beam, one fiber transmitted the collected light back to the laboratory and one fiber collected laser light scattered inside the probe. This light was used as a reference to correct the Raman signal for fluctuations in the delivered laser beam. The fiber was coupled to a diode located near the data reduction equipment. An electronic circuit with variable low pass filters (here a 10 Hz filter was used to remove the 400 Hz laser beam modulation used for lock-in detection) and an amplifier bank created an electronic signal that was proportional to the laser light.

Calibration Measurements. Because of the abundance of nitrogen in air, a readily available calibration source, initial experiments were centered around the nitrogen Raman spectrum. A series of scans are shown in Figure 7. Each scan represents the spectral range from 5780 to 5920 Angstroms. This range was scanned repeatedly. The initial ten scans were conducted with a scan rate of 0.2 Angstrom/s, and an amplifier time constant of 30 s. To traverse a single such scan therefore took 700 s, with a 8 s transition time between scans.

This accumulative time is displayed on the horizontal axis, while the vertical axis indicated the real-time intensity. The subsequent 37 scans had a scan rate of 1 Angstrom/s and a time constant of 3 s. Each traverse for these scans took 140 s.

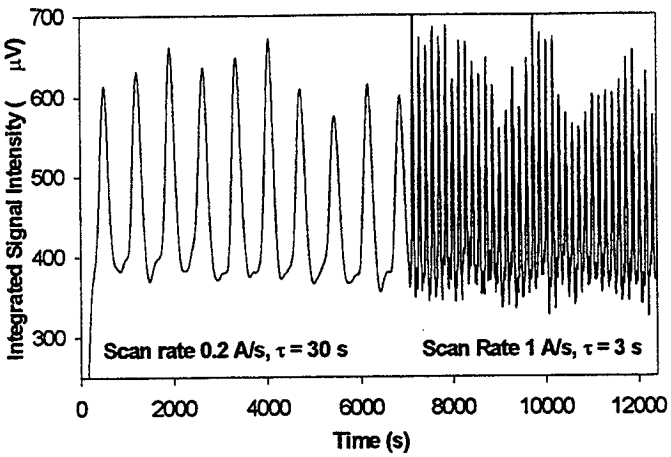

Fig. 7: Repeated nitrogen Raman spectra for two sets of scan rate / time constant

The peak values of the slow time constant scans were lower due to the longer amplifier integration time, and the peak to peak fluctuations were less than for the faster time constant scans. However, the response was slower by an order of magnitude. The peak values (which translates in dynamic range) were better for the faster scans. This advantage will not be important for the continuous monitoring of the peak value, where the spectrometer is set at the peak value, and thus the average over time will be the full peak value. The figure clearly shows a good detectability of nitrogen in air.

Figure 7 also clearly highlights the problem for this measurement. There are significant fluctuations from peak to peak, which give a significant uncertainty in the exact value. The fluctuations can be reduced by choosing a longer time constant. But this goes at the expense of the response, which increases from seconds to minutes. One approach to reduce the fluctuations is to compensate the signal intensity for the fluctuations in laser power delivered at the probe. Thereto a fiber was embedded inside the optical probe that collected scattered laser light and transmitted it to the data acquisition equipment. There the fiber was coupled into a diode which monitored the light fluctuations and converted this into a proportional voltage. The diode circuit contained a variable short pass filter to remove the modulation from the laser light, and a variable amplifier. To date, results of these tests have not been satisfactory. An improved correction circuit needs to be implemented.

The next step was to verify that the system parameters had not changed from the laboratory setup. An important calibration of the system consisted of the measurement of the oxygen and nitrogen in air. To that end, a calibration mixture of 21% O_2, 78% N_2, and 1% of Ar was inserted at ambient pressure and temperature inside the sample vessel. Previous laboratory calibration measurements were obtained by subtracting the background obtained in a vacuum from the spectrum obtained in air and comparing the peaks of nitrogen and oxygen in air. In this in-situ measurement, obtaining a background in a vacuum was not possible. The oxygen peak could be obtained, however, by subtracting the endothermic gas spectrum from the air spectrum, because oxygen was not expected to be a significant endogas constituent. Nitrogen was a constituent in both spectra. Therefore, the nitrogen spectrum could not be extracted through this process but was obtained by subtracting an artificial background from the air spectrum. The resulting calibration spectrum, with and without subtracted background, is shown in Figure 8.

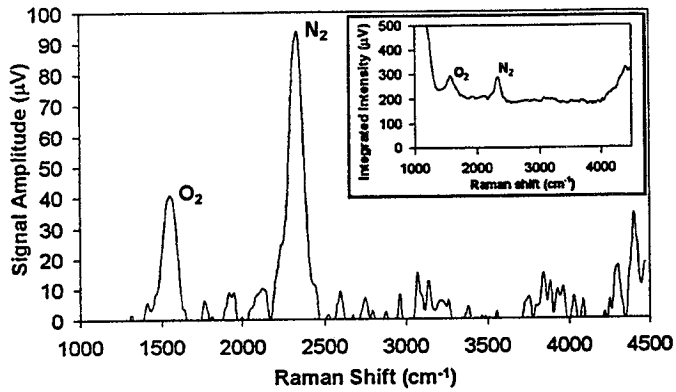

Fig. 8: Calibration spectrum of air inside sample vessel.

This figure shows that the background with the 150 ft fiber was significantly stronger than with the 12 ft fiber as shown in Figure 4. It was also clear that the signal was weaker due to the loss in power during transmission. From these oxygen and nitrogen peak intensities and the given percentages of both species, it was possible to extract the relative intensities. The ratio of intensities of oxygen and nitrogen for equal number densities extracted from this measurement was 1.615 which compared extremely well with the value obtained in the laboratory for this value (see Table I). This gave us confidence in the measurement.

Because carbon monoxide was the species to be monitored and nitrogen was the calibration species, it was important to observe the transition of the CO-N_2 spectrum from air to endogas during the startup of the generator. An advantage of this monitoring was that the CO and N_2 peaks are closely spaced, such that a spectral scan from 5680 A to 5920 A covered both peaks. With a scan rate of 1 A/s, such a traverse took 4 minutes to completion.

Figure 9 shows a series of such scans at the startup of the generator, during the transition from air to endogas mixture. The lock-in amplifier time constant used was 3 s. The horizontal axis displays the time history, the vertical axis

shows the signal intensity. Each scan took 4 minutes, with a spectrometer reset to the beginning of the spectral range of about 8 s. The first ten scans were in air, where the peaks represented the nitrogen. The peak to peak fluctuation and background noise were significant due to the fast time constant used. The sequence following the air scans represented the start-up of the generator. For about twelve minutes after startup, the spectrum was vague, and no useful data could be obtained from the signal. Thereafter, the signal became more defined and clear carbon monoxide and nitrogen peaks could be observed.

The insert of Figure 9 shows the average of 20 spectra of carbon monoxide and nitrogen during the endothermic gas scans under startup conditions. The horizontal axis shows the wavelength. Two features were noticed. At the lower wavelength from the carbon monoxide, some signal was noticed, of which the source is not known. This was not observed in subsequent scans. Therefore it was thought to be part of the generator startup sequence. It could also be seen that the carbon monoxide concentration was higher than expected. A simple calculation showed this concentration to be 29.2 ± 7.1 %, much higher than anticipated and with a large uncertainty. The dew point was not recorded for these measurements. No conclusion could therefore be made concerning this result. It is known however, that an endothermic gas generator needs a substantial amount of time to stabilize after start up.

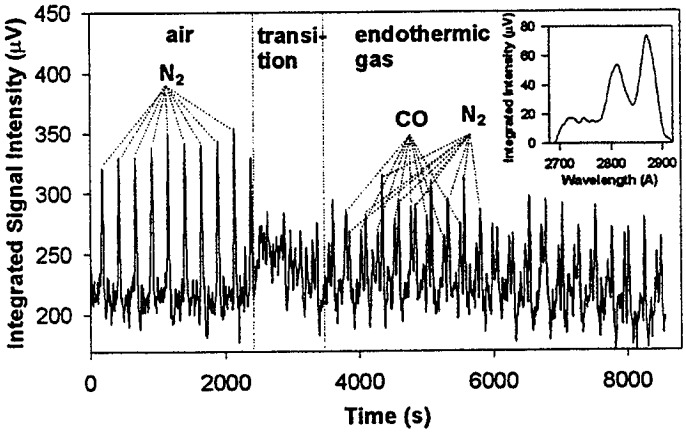

Fig. 9: Transition from air to endothermic gas during generator start-up. Insert: average of endothermic gas scans.

Using the calibration data described in the previous section, it was possible to measure and monitor the species densities inside the endothermic gas. The endothermic gas spectrum was obtained with a dew point setting of 28. Both the spectrum without and with background subtraction are given in Figure 10. This spectrum with background subtraction was obtained by subtracting the air spectrum from the endogas spectrum, with the exception of the nitrogen peak, where an artificial background was subtracted.

Easily identifiable species in Figure 10 are carbon monoxide, nitrogen and hydrogen. Water appears relatively strong also. This species was not characterized in the laboratory tests. The relative strength of the Raman line of water at 3652 cm^{-1} is found in literature[12] to be 3.4 for specific polarization and geometry, and is given in the last column of Table I. This is not likely to be exact for the conditions in this experiment, but is the only available option at the moment. A very weak carbon dioxide2 peak can be detected, but the signal is close to the noise level. A number of peaks identified can be ascribed to methanol (CH_3OH), but because this species was not mentioned before, and because it is not sure whether the peaks are caused by methanol, the species is indicated between parenthesis and will not be considered in the species calculation.

With the relative intensities listed in Table I, it is now possible to calculate the percentage of each species from the endothermic gas spectrum. The results are given in Table II. The carbon dioxide values are the only two peaks from the same species. the peak at 1285 indicates a CO_2 percentage of 1.64 ± 1.121 % and the peak at 1388 indicates a concentration of 1.88 ± 1.17 %, for an average of 1.76 ± 1.19 %. The other species concentrations are straightforward.

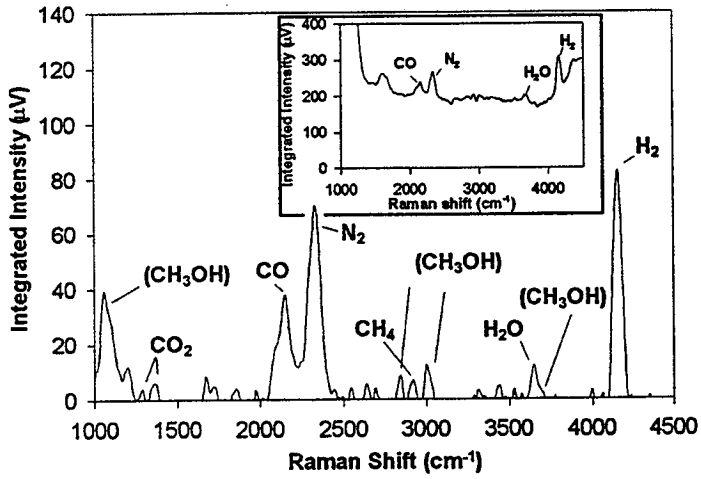

Fig. 10: Raman spectrum of endothermic gas observed at the generator.

The desirable concentrations of the endothermic gas are 20% CO, 40% N_2, and 40% H_2 with little or no methane or carbon dioxide. Low carbon dioxide concentration is desired so as not to block carbon penetration at the solid surface due to saturation of carbon. The relatively high carbon dioxide, high N_2, and high carbon monoxide concentration, as well as the low hydrogen concentration and the presence of water seem to indicate too much air in the air/methane input to the generator.

The numbers in the last column are made to add up to 100% of the endogas. A calculation was made that calculated the percentages of each species based on the oxygen line intensity of the air reference spectrum. The results are shown in the last column of Table II. For this absolute calculation, the numbers add up to 130% of endogas, which is a significant overcalculation. A number of variables have not been included however, such as fiber attenuation at different wavelengths, which could account for the overprediction.

Carbon Monoxide Monitoring. All measurements described thus far were needed to verify the repeatability of the instrument under different circumstances. It also was necessary to verify the repeatability after dis- and re-assembly of the equipment, and the instrument capability under less than ideal environment, such as in a steel treating plant. In view of the experimental conditions, the results were within acceptable limits.

In order to monitor the carbon monoxide concentration, a first test was needed to establish the exact spectral location of the carbon monoxide peak. A test was conducted where the carbon monoxide and nitrogen spectra were monitored with a scan rate of 1 Angstrom/s and a time constant of 3 seconds. A time history of that experiment is shown in Figure 11. The carbon monoxide peak appeared around 5792 Angstrom. With a time constant of 3 s, the lock-in amplifier signal displayed a time delay of about 10 to 15 s, in which the spectrometer scanned with 1 Angstrom/s. The exact spectral location of the peaks was therefore somewhere between 5778 and 5783 Angstrom. For these tests, a trial and error method was used to locate the peak, after which it was still not certain that the peak was located accurately. An advantage of the instrument is, however, that a small offset from the peak location still gives a good monitorable signal. After locating the spectral peak, the spectrometer was fixed at that position and after a few minutes of observation with a 3 s time constant, this was changed to 30 s to reduce the fluctuations. This change, however, reduced the response from 10 s to 2 minutes.

Table II: Measured species concentrations, both relative and absolute values

species	spect. locat. (A)	intensity relat. to N_2	relative % of endothermic gas	absolute % based on calibration
CO_2	1284 1373	1.59 2.05	1.61±1.21 1.84±1.17	2.10±1.58 2.41±1.31
CO	2117	1.10	21.39±3.79	27.97±4.96
N_2	2316	1.00	43.68±4.01	57.12±5.24
CH_4	2905	7.47	0.59±0.44	0.77±0.57
H_2O	3648	3.4	2.22±1.89	2.91±2.48
H_2	4148	1.69	30.39±3.37	39.74±4.41

Figure 11 shows a first effort in actually monitoring the signal of carbon monoxide. The figure indicates the time history of finding the peak value and the adjustment of the measurement variables, such as the time constant (t). After obtaining the peak location, it was found that the accuracy of the carbon monoxide concentration that can be observed for this first trial was 21.38% with a 17.63% to 25.59% peak to peak fluctuation.

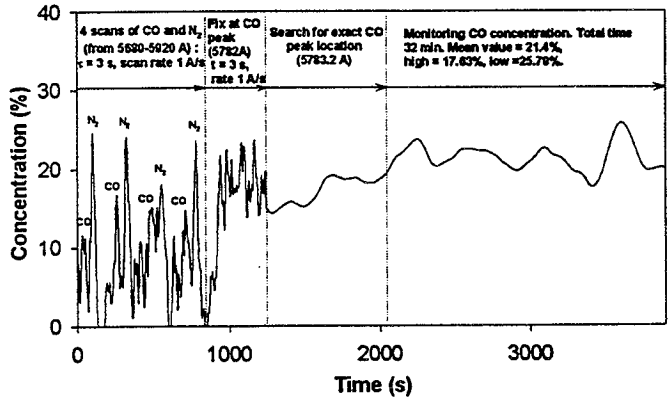

Fig. 11: Time history of finding carbon monoxide peak value

A few subsequent tests showed similar results. As a last test it was decided to observe the signal while changing the dew point of the gas generator. Changing dew point implies a change in carbon dioxide concentration, but no change in carbon monoxide should occur. The results of that test are shown in Figure 12. During the first ten minutes of the experiment, the dew point was set to 28. The CO percentage was determined at 21.4%. After ten minutes, the dew point was set to 55. Initially it looked as if the CO percentage measured decreased. After a few minutes, however, the CO concentration measured showed a return to the original level. The average value of CO during this 22 minute period was 21.5%, with a high of 23.1% and a low of 19.7%. thus only slightly higher than the first ten minutes. But no effect of a change in dew point was noticed.

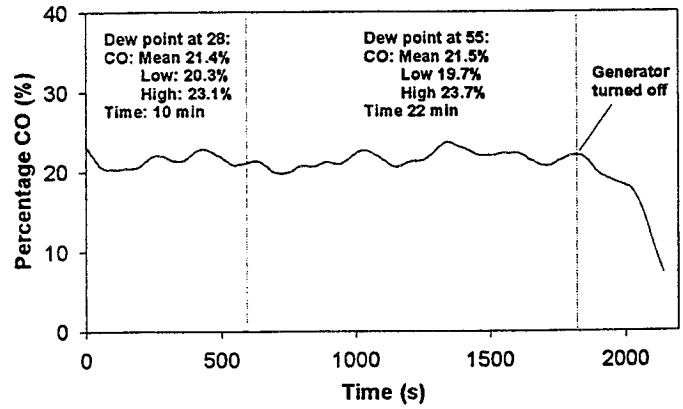

Fig. 12: Effect of change in carbon monoxide concentration on monitor signal

At the end of this test, the generator was turned off. Within six minutes, the CO percentage had dropped to 7.1%. The slow drop in CO content was not only due to the slow response of the instrument, but also to the fact that after the generator was turned off, the gas inside the sample vessel was displaced only gradually, thus the reduction in CO took place gradually, closely monitored by the instrument. The extend to which the monitoring followed the reduction in CO could therefore not be established. The detection of this drop in CO was a successful demonstration of the capability of this instrument to monitor species concentrations.

Summary and Recommendations

A real time, in-situ, non-intrusive instrument was designed and build to detect, identify and monitor gaseous constituents in an endothermic gas atmosphere. Calculations showed the feasibility of such an instrument, based on Raman scattering. Laboratory tests were performed that proved the concept to be valid. After some small modifications, the instrument was field tested in a steel treating plant, where it was installed to analyze the composition of an endothermic gas near the gas generator and to monitor the carbon monoxide concentration. Successful tests were performed that showed the applicability of this technology to monitor the gaseous constituents.

Carbon monoxide, carbon dioxide, methane, water, nitrogen, and hydrogen were detected and quantified. Carbon monoxide monitoring over periods of 30 minutes showed a stable mean of around 21.4% with peak to peak fluctuations from 17.5 to 25.5 %. Changes in carbon monoxide concentration due to changes in dew point setting of the generator were not detected. A change in carbon monoxide concentration due to the turning off of the generator was closely monitored.

In order to make this device more attractive for commercial applications, improvements in accuracy and speed will be needed over this proof-of-concept system. A number of improvements have been identified. First, increasing the diameter of the delivery fiber, allows more laser power to be transported and causes the laser intensity to exhibit less fluctuations. Second, an optical isolator used to separate the laser output coupler from the fiber surface was found to cause a gradual drift in laser fiber coupling. Solidifying the optics inside the optical isolator or the use of an improved isolator will eliminate this drift. Third, an improved compensation system for corrections of fluctuations in delivered laser power will improve signal to noise ratio (SNR). Fourth, optimization of the optics, such as the dichroic filter and pass filters, as well as a redesign of the probe head itself will reduce scattered light inside the optics and improve the SNR. This redesign will also reduce interference of stimulated Raman and fluorescence from optical components. And finally, an improved detection mechanism, such as the use of sensitive Gallium-Arsenide tubes, and deeper cooling will reduce the noise.

Optimizing for accuracy and response will have the current infrared technology as a benchmark. The advantages of in-situ measurement, lack of need for in-line calibration, and multiple species monitoring market advantages. A cost analysis of a working commercial device has to be made in order to judge the value of this device as compared to existing instruments.

Tests thus far were performed on the endothermic gas near the generator. The next logical step is to adapt the device for measurement of the gases inside the furnace, where the remote capability will allow actual atmosphere measurements without the need for probe insertion.

The field tests were performed on a carburizing atmosphere. The device is not limited to those furnaces, however. Nitriding furnaces, nitrocarburizing furnaces, and basic oxygen furnaces among others, can benefit from this technology.

Acknowledgment

The author would like to acknowledge Joe Powell from Akron Steel Treating, Inc. for the use of his facilities and expertise to perform the described tests.

References

[1] Haga, L.J., "Process Control: surface protection, and endothermic atmospheres," From *Heat Treating*, February 1989, pp. 22-23.

[2] Ziegler, J. C., "Computer Analysis of Carbon Behavior in Carburizing Atmospheres," Heat Treating Magazine.

[3] McCurdy, D.W., " Improving the Accuracy of Oxygen Probe Control Systems," Proc. Intl. Heat Treating Conference, Schaumburg, IL, April 18-20, 1994, pp117-121.

[4] Lapp, M. and Penney, C.M., "Raman Measurements on Flames," From *Advances in Infrared and Raman Spectroscopy* (R.J.H. Clark and R.E. Hester, Ed.), Chap. 6, Heyden, London, 1977.

[5] Lederman, S.,"The Use of Laser Raman Diagnostics in Flow Fields and Combustion," *Progress in Energy Combustion Science*, Vol.3, 1977, pp 1-34.

[6] de Groot, W.A., "The Development of a Fiber Optic Raman Temperature Measurement System for Rocket Flows", AIAA Paper 91-2316, Sacramento, CA, 1991.

[7] de Groot, W.A. and Weiss, J.M., "Species and Temperature Measurement in H_2/O Rocket Flow Fields by Means of Raman Scattering Diagnostics", AIAA Paper 92-3353, Nashville, TN, 1992.

[8] de Groot, W.A., and Zupanc, F.J., "Laser Rayleigh and Raman Diagnostics for Small Hydrogen/Oxygen Rockets," SPIE Paper 1862-10, Los Angeles, CA, 1993

[9] de Groot, W.A. and Tsuei, H.H., "Gaseous Hydrogen/Oxygen Injector Performance Characterization," AIAA Paper 94-0220, Reno, NV, 1994.

[10] de Groot, W. A., "The Use of Spontaneous Raman Scattering for Hydrogen Leak Detection," AIAA 94-2983, Indianapolis, IN, June 27-29, 1994.

[11] de Groot, W.A., "Fiber-Optic Based Compact Gas Leak Detection System," AIAA Paper 95-2646, San Diego, 1995.

[12] (a) Schroetter, H.W., and Kloeckner, H.W., "Raman Scattering Cross Sections in Gases and Liquids," *Raman Spectroscopy of Gases and Liquids* (A. Weber, Ed.) Topics in Current Physics: Springer Verlag, 1979.

REPORT DOCUMENTATION PAGE

Form Approved
OMB No. 0704-0188

1. AGENCY USE ONLY (*Leave blank*)	2. REPORT DATE	3. REPORT TYPE AND DATES COVERED
	January 1997	Final Contractor Report

4. TITLE AND SUBTITLE
Potential New Sensor for Use With Conventional Gas Carburizing

5. FUNDING NUMBERS
WU–242–70–02
C–NAS3–27186

6. AUTHOR(S)
W.A. de Groot

7. PERFORMING ORGANIZATION NAME(S) AND ADDRESS(ES)
NYMA Inc.
2001 Aerospace Parkway
Brook Park, Ohio 44142

8. PERFORMING ORGANIZATION REPORT NUMBER
E–10576

9. SPONSORING/MONITORING AGENCY NAME(S) AND ADDRESS(ES)
National Aeronautics and Space Administration
Lewis Research Center
Cleveland, Ohio 44135–3191

10. SPONSORING/MONITORING AGENCY REPORT NUMBER
NASA CR–202306

11. SUPPLEMENTARY NOTES
Prepared for the 16th International Heat Treating Society Conference and Exposition sponsored by the American Society for Metals, Cincinnati, Ohio, March 19–21, 1996. Project Manager, Steven J. Schneider, Space Propulsion Technology Division, NASA Lewis Research Center, organization code 5300, (216) 977–7484.

12a. DISTRIBUTION/AVAILABILITY STATEMENT
Unclassified - Unlimited
Subject Category 20

This publication is available from the NASA Center for AeroSpace Information, (301) 621–0390.

12b. DISTRIBUTION CODE

13. ABSTRACT ***(Maximum 200 words)***

Diagnostics developed for in-situ monitoring of rocket combustion environments have been adapted for use in heat treating furnaces. Simultaneous, in-situ monitoring of the carbon monoxide, carbon dioxide, methane, water, nitrogen and hydrogen concentrations in the endothermic gas of a heat treating furnace has been demonstrated under a Space Act Agreement between NASA Lewis, the Heat Treating Network, and Akron Steel Treating Company. Equipment installed at the Akron Steel Treating Company showed the feasibility of the method. Clear and well-defined spectra of carbon monoxide, nitrogen and hydrogen were obtained by means of an optical probe mounted on the endothermic gas line of a gas generator inside the plant, with the data reduction hardware located in the basement laboratory. Signals to and from the probe were transmitted via optical fibers.

14. SUBJECT TERMS	15. NUMBER OF PAGES
Gas monitoring and control; Fiber optics; Raman scattering	12
	16. PRICE CODE: A03

17. SECURITY CLASSIFICATION OF REPORT	18. SECURITY CLASSIFICATION OF THIS PAGE	19. SECURITY CLASSIFICATION OF ABSTRACT	20. LIMITATION OF ABSTRACT
Unclassified	Unclassified	Unclassified	